Earthq Eng & Eng Vib (2014) 13: 583-597 **DOI**:10.1007/s11803-014-0265-6

A European digital accelerometric database: statistical analysis of engineering parameters of small to moderate magnitude events

Carlos S. Oliveira[1†], Gerard Gassol[2‡], Xavier Goula[2§] and Teresa Susagna[2*]

1. *Instituto Superior Técnico, Universidade de Lisboa, Lisboa, Portugal*

2. *Institut Cartogràfic i Geològic de Catalunya, Barcelona, Spain*

Abstract: During the NERIES Project, an accelerometric database containing European digital information was developed. Besides event and station metadata, ground motion parameters, computed in a homogeneous manner, were assembled: PGA, PGV, AI, TD, CAV, HI and PSV(*f*,5%) (19,961 components, 2629 events, 547 stations). Merging small and moderate magnitude events produced a unique database capable of providing important information such as: (i) Correlations between several ground motion parameters follow analogous trends as in previous worldwide datasets, with slight corrections. (ii) Although PGA attenuations with distance show great uncertainties, four recent GMPEs recommended for Europe fit quite well the central 50% data interval for the distance range $10 < R < 200$ km; outside these distances, they do not fit. (iii) Soil amplification ratios indicate that weak motion (low magnitudes and larger distances) shows larger amplification than strong motion (short distances and large magnitudes) as represented in UBC97 for the USA, but not in EC8 for Europe. (iv) Average spectral shapes are smaller than in the EC8. (v) Differences in amplification factors for PGA, PGV and HI for EC8 soil classes B and C, and differences in spectral shapes for these soil classes, indicate that EC8, Type 2 S-coefficient should be frequency dependent, as in UBC97.

Keywords: NERIES project; parametric accelerometric database; European region; PGA; EC8; soil amplification

1 Introduction

Currently, European earthquake strong motion data are made available by numerous individual European networks, namely, Çagnan *et al.* (2011) for Turkey, IGN (1999) for Spain, Luzi *et al.* (2008) for Italy, Margaris *et al.* (2010) for Greece, Péquegnat *et al.* (2008) for France, Vilanova *et al.* (2009) for Portugal and Wyss (2004) for Switzerland. Additional compilations are provided by Ambraseys *et al.* (2004), Douglas *et al.* (2006) and ESD (2013). Various organizations such as COSMOS (Archuleta *et al.*, 2006), K-Net (Kinoshita, 2003) and CWB of Taiwan (Shing *et al.*, 2003) present updated information for different regions of the world.

In the absence of an archive for recent digital European data, the NERIES Project (2006−2010), acting under a Networking Activity (NA5), aimed at developing a distributed accelerometric database to provide open waveform data and other topics to the scientific and engineering communities. This effort covered strong motion (SM) activity for the period 1996-2010. To achieve this goal, several tasks were developed by the agencies participating in the NERIES Project (ICGC, Institut Cartogràfic i Geològic de Catalunya, former IGC; IST, Instituto Superior Técnico; ISTerre/RAP, Institut de Sciences de la Terre/ Réseau Accélérometrique Permanent; KOERI, Kandilli Observatory and Earthquake Research Institute; ITSAK, Institute of Engineering Seismology and Earthquake Engineering; and ETHZ, Swiss Federal Institute of Technology): (i) a detailed characterization of the recording instruments and the sites of the accelerometric stations; (ii) the development of computer software (PARAMACC) for data treatment to determine, in a homogenized manner, a collection of waveform parameters; and (iii) the development of a webportal (Earthquake Data Portal, 2011) to present event metadata (EMSC-CSEM, 2011) and permit the access of users to retrieve parameter and waveform data (Roca *et al.*, 2011; Péquegnat *et al.*, 2011).

These parameters and waveforms are important for improving the characterization of ground motion, and are used in earthquake engineering for the analysis of structural behavior, including damage assessment for risk mitigation.

Part of this information was compiled in an "events-

Correspondence to: Carlos Sousa Oliveira, Instituto Superior Técnico, Universidade de Lisboa, Av Rovisco Pais 1, 1049-001 Lisbon, Portugal
Tel: +351 218418219
E-mail: csoliv@civil.ist.utl.pt
†Professor; ‡Engineer; §Chief Researcher; *Associate Researcher

Supported by: EC Project NERIES, Sixth Framework Programe, Contract No. RII3-CT-2006-026130
Received December 10, 2013; **Accepted** October 19, 2014

stations-ground-motion parameters" table (Gassol, 2011), containing accelerometric data recorded in different stations. Besides earthquake data (magnitude and epicentral distances), and data related to recording stations and soil conditions, this table contains waveform parameters (PGA, PGV, AI, TD, CAV and HI, together with PSV(f,5%) for 28 frequencies), which were computed by each agency using PARAMACC.

The main purpose of this paper is to analyze statistically the tendencies presented by ground motion parameters, considering either the entire data-set or analyzing the data by classes of magnitude, epicentral distance or soil conditions, and then separating the data by agency.

The data assembled as of December 2010 refer to records since 1993 that belong to the above mentioned six different European networks, plus a set of Italian (Italian Accelerometric Archive – ITACA, 2010) and Spanish data (Instituto Geográfico Nacional – IGN, 2010). Initially, approximately 12,300 3-component records from 1026 stations associated with 3474 events, characterized by magnitude (M_L1–7.4) and epicentral distances (0–863 km), were assembled in this prototype (Earthquake Data Portal, 2011). When available, the soil conditions associated with each station were included.

This large but incomplete set comprises different situations, related to event size, epicentral distances and soil conditions. As recently noted by Delavaud *et al.* (2012) and Atkinson (2012), by merging small with moderate magnitude events, including a few large magnitude events, we obtain a unique database for the European region capable of providing information on many seismological characteristics of ground motion data.

The contents of this database can be considered a representative sample of the Euro-Mediterranean region, even though large magnitudes (M > 6) events are not well represented in all regions due to the short period of available digital data and, consequently, to the constraints imposed by the Richter law of occurrences.

After the conclusion of NERIES, other on-going projects, ORFEUS (2013) and EMSC-CSEM (2013), are being developed to continue the efforts to collect SM information and store waveform data. The latest developments led to the beta version of the Rapid Raw Strong Motion (RRSM, 2014) system, which automatically aims at delivering strong motion products in near-real-time for earthquake scientists and earthquake engineers. For sure, these new projects will enhance the results presented herein. Information for larger magnitude events will be greatly enriched if complementary data with more accurate definitions of tectonic environment, style-of-faulting, magnitude description, distance station-fault, soil conditions, etc. becomes available.

2 Data sets and parameter definitons

Figure 1 shows: (a) a map with the location of the stations (IGC, IST, RAP, KOERI, ITSAK, ETHZ, ITDPC and IGN) and (b) the events recorded by the stations.

As a main feature of the data processing within PARAMACC, we should emphasize that the acceleration time history, $a(t)$ in cm/s^2, was baseline corrected by a one-degree polynomial approximation, fitted with a least squares algorithm and high-pass filtered with a Butterworth IIR of two poles with a cut-off frequency of 0.1 Hz, for all records. This choice, which reflects the wide variety of instrument types and resolution in the selected networks, maintains homogeneity and consistency, and avoids excessive restrictions. Filtering was applied both in the forward and reverse time directions to avoid phase distortion. Data padding was introduced to avoid low-frequency contamination. A number of zeros equivalent to 5% of the time duration was added, both at the beginning and at the end of the

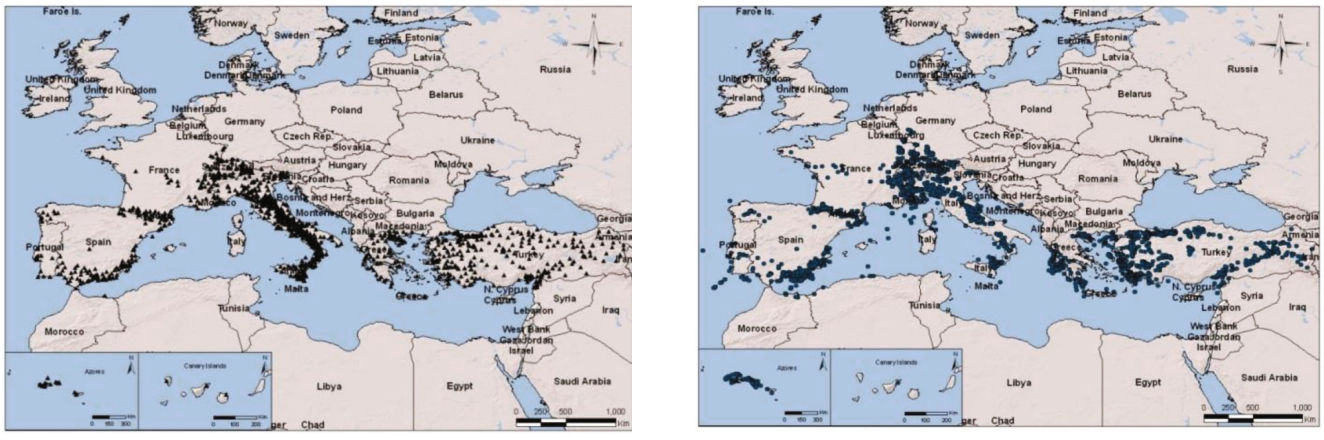

(a) (b)

Fig. 1(a) European station distribution providing preliminary data (courtesy S. Godey, 2010); (b) Epicentres of recorded events (courtesy S. Godey, 2010)

signal. No tapering was applied (Boore and Akkar, 2003; Akkar and Bommer, 2006).

The following waveform parameters were obtained and stored in the "events-stations-ground-motion parameters" table (Lee *et al.*, 2002):

• PGA: Peak Ground Acceleration, in cm/s^2, is directly obtained from the maximum absolute value of the filtered acceleration time-history $a(t)$; it is the most common parameter used in earthquake engineering; usually utilized for scaling the standard spectra for period equals to zero;

• PGV: Peak Ground Velocity, in cm/s, is obtained from the maximum absolute value of the calculated velocity time-history, $v(t)$; it is an alternative measure, which reflects the damage to pipelines, building contents and nonstructural elements;

• AI: the Arias Intensity, in cm/s; a specific function related to the energy content (Arias, 1970); often used as an indicator of Macroseismic Intensity (Cabañas *et al.*, 1997);

$$\mathrm{AI} = \frac{\pi}{2 \cdot \mathrm{g}} \int_0^{\infty} a^2(t)\mathrm{d}t$$

• TD: Trifunac Duration is the time interval, in s, between 5% and 95% of the Husid function (Husid, 1973);

$$\mathrm{Husid}(t) = \frac{\int_0^{t} a^2(t)\mathrm{d}t}{\int_0^{\infty} a^2(t)\mathrm{d}t}$$

• CAV: Cumulative Absolute Velocity, in cm/s; this integral function has been recently related to structural damage (Kramer, 1996);

$$\mathrm{CAV} = \int_0^{\infty} \left|a(t)\right| \mathrm{d}t$$

• PSV(f, 5%) 5% damping: Pseudo-Velocity Response Spectrum, in cm/s, computed for 28 frequencies equally spaced logarithmically from 0.15 to 39 Hz. For weak motions (PGA < 0.01 g or PGV < 1 cm/s), we only considered spectral values for frequencies > 0.5 Hz.

• HI: Housner Intensity, in cm (Housner, 1952). This is the time integral of a ξ = 5% damped PSV calculated between 0.1 and 2.5 s, and gives a measure of the potential damage of the accelerogram for typical engineered structures:

$$HI\ (\xi) = \int_{0,1}^{2,5} \mathrm{PSV}(T, \xi)\mathrm{d}T$$

The "events-stations-ground-motion parameters" Table, created to perform a complete analysis of the data, assembles all the information gathered in different working areas from event characterization and station soil conditions, to waveform parameters (Gassol, 2011). An illustration of the contents of this table is presented in Table 1. Each row of the table lists all of the information for each individual component. Updating the table can be easily performed when new data become available. The whole table can be downloaded from www.icgc.cat.

The "events-stations-ground-motion parameters" Table was subjected to a detailed evaluation process to check the quality of the data and identify the most obvious errors made during the assemblage of data, such as wrong event locations, records with poor signal/noise ratios, and records with erroneous units (e.g., cm/s^2 instead of tenths of g), etc.

From the initial data, we retained only events with $M > 3$ to eliminate the ones with low signal-to-noise ratios; we also separated the Azores Islands from South Portugal (S.P.) in the IST records (Gassol, 2011).

This selection lead to 19,961 components from 2,629 events recorded in 547 stations. A simple classification of the soil conditions associated with each station (Rock-R, Hard-H, and Soft-S) was available for all of the contributing agencies. However, for approximately 60% of the data (ISTerre/RAP, KOERI, IGN and ITDPC - Dipartamento della Protezione Civil Italiana networks - corresponding to 12,288 components), we also dispose the soil classification based on EC8 (2004) Classes (A, B, C, D and E). These records (Table 2) are indicated by network, with reference to the time interval of events and the range of magnitudes.

As Table 2 clearly expresses, events were not recorded equally by agencies or stations. Whereas IST (South Portugal) and IGC contributed with a small number of components (less than 200), ISTerre and KOERI (with more than 5,000 each) contributed with more than half of the total number of components.

To illustrate the importance of the assembled dataset, Fig. 2 shows the distribution of the PGA values of records on a magnitude−distance plot. The entire analysis was performed based on the arithmetic average of both horizontal components. The colors of the dots are different for different bins of PGA values. It is clear that this large quantity of data points, covering a wide range of magnitudes and epicentral distances, is of great importance to check the attenuation phenomenon, especially for magnitudes up to M6. Similar trends can be observed in the plots of the other computed parameters.

3 Analysis of the computed parameters

In the following sections, we first analyze the correlations between different pairs of accelerometric parameters; next, we study the dependence of PGA and the other parameters on magnitude and epicentral

Table 1 Events-stations-ground-motion parameters Table. Example with a few records (Record-register: identification header; Network; Comp; Station code; Date; Longitude; Latitude; M_l: Local magnitude; PGAU: Uncorrected PGA (cm/s^2); PGAC: Corrected PGA, (cm/s^2); AI: Arias intensity (cm/s); TD: Trifunac duration (s); CAV: Cumulative absolute velocity (cm/s); PGV (cm/s); HI: Housner intensity (cm); DEpi: Epicentral distance (km); PSV(f) 5% damping for 28 frequencies (from 0.15 Hz to 39 Hz); Soil type R,H,S; EC8 Soil Class A, B, C, D, E from geology; EC8 Soil Class A, B, C, D, E from Vs30; Vs30 value. (x and O means no data)

Register	Network	Comp.	Station	Date	Longitude	Latitude	M_l	PGAU	PGAC	AI	TD	CAV	PGV	HI	DEpi (km)
19960105.034320.LGAR-IST.01.HNE.asc	Azo	E	LGAR	05/01/1996	-27.12	38.54	4.4	17.40	17.40	0.1756	9.23	34.94	0.61	0.86	16.24
19960105.034320.LGAR-IST.01.HNN.asc	Azo	N	LGAR	05/01/1996	-27.12	38.54	4.4	9.74	9.74	0.0830	14.92	25.90	0.23	0.37	16.24
19960105.034320.LGAR-IST.01.HNZ.asc	Azo	Z	LGAR	05/01/1996	-27.12	38.54	4.4	14.87	14.87	0.1415	9.60	31.54	0.52	0.99	16.24
20030504.133008.1201-KOE.01.HNE.asc	KOE	E	1204	04/05/2003	40.44	39.00	3.8	6.33	6.34	0.0159	6.79	8.77	0.31	0.45	12.68
20030504.133008.1201-KOE.01.HNN.asc	KOE	N	1204	04/05/2003	40.44	39.00	3.8	3.00	2.99	0.0098	8.69	7.83	0.19	0.29	12.68
20030504.133008.1201-KOE.01.HNV.asc	KOE	V	1204	04/05/2003	40.44	39.00	3.8	3.54	3.53	0.0092	7.83	7.14	0.10	0.22	12.68
20020417.064254.RSN-ITD.01.ENE.asc	ITD	E	RSN	17/04/2002	16.87	39.68	4.7	65.57	65.57	1.3201	2.74	61.10	2.86	3.99	23.85
20020417.064254.RSN-ITD.01.ENN.asc	ITD	N	RSN	17/04/2002	16.87	39.68	4.7	34.51	34.51	0.99	4.45	61.09	1.24	2.44	23.85
20020417.064254.RSN-ITD.01.ENZ.asc	ITD	Z	RSN	17/04/2002	16.87	39.68	4.7	10.87	10.87	0.11642	7.80	24.52	0.51	0.92	23.85
20040621.231002.STDM-RAP.00.ENE.asc	RAP	E	STDM	21/06/2004	7.67	47.50	3.8	3.77	3.77	0.0053	7.34	5.25	0.08	0.05	94.66
20040621.231002.STDM-RAP.00.ENN.asc	RAP	N	STDM	21/06/2004	7.67	47.50	3.8	3.82	3.82	0.0054	8.07	5.37	0.06	0.05	94.66
20040621.231002.STDM-RAP.00.ENZ.asc	RAP	Z	STDM	21/06/2004	7.67	47.50	3.8	1.66	1.66	0.0017	19.14	3.66	0.03	0.02	94.66

Register	PSV 0.15 Hz					PSV 0.5Hz	...20 freq...	PSV 39 Hz	RHS	EC8- geology	EC8-Vs30	Vs30 (m/s)
19960105.034320.LGAR-IST.01.HNE.asc	xxxxx	xxxxx	xxxxx	xxxxx	xxxxx	0.12	...	0.06	S	O	O	O
19960105.034320.LGAR-IST.01.HNN.asc	xxxxx	xxxxx	xxxxx	xxxxx	xxxxx	0.06	...	0.03	S	O	O	O
19960105.034320.LGAR-IST.01.HNZ.asc	xxxxx	xxxxx	xxxxx	xxxxx	xxxxx	0.15	...	0.06	S	O	O	O
20030504.133008.1201-KOE.01.HNE.asc	xxxxx	xxxxx	xxxxx	xxxxx	xxxxx	0.09	...	0.01	H	O	B	528.7
20030504.133008.1201-KOE.01.HNN.asc	xxxxx	xxxxx	xxxxx	xxxxx	xxxxx	0.06	...	0.01	H	O	B	528.7
20030504.133008.1201-KOE.01.HNV.asc	xxxxx	xxxxx	xxxxx	xxxxx	xxxxx	0.06	...	0.01	H	O	B	528.7
20020417.064254.RSN-ITD.01.ENE.asc	0.19	0.24	0.29	0.34	0.39	0.48	...	0.20	R	A	O	O
20020417.064254.RSN-ITD.01.ENN.asc	0.08	0.16	0.21	0.35	0.44	0.50	...	0.12	R	A	O	O
20020417.064254.RSN-ITD.01.ENZ.asc	xxxxx	xxxxx	xxxxx	xxxxx	xxxxx	0.15	...	0.04	R	A	O	O
20040621.231002.STDM-RAP.00.ENE.asc	xxxxx	xxxxx	xxxxx	xxxxx	xxxxx	0.01	...	0.011	S	O	E	O
20040621.231002.STDM-RAP.00.ENN.asc	xxxxx	xxxxx	xxxxx	xxxxx	xxxxx	0.01	...	0.011	S	O	E	O
20040621.231002.STDM-RAP.00.ENZ.asc	xxxxx	xxxxx	xxxxx	xxxxx	xxxxx	0.01	...	0.001	S	O	E	O

Table 2 Number of accelerograms (components) assembled in the "Events-stations-ground-motion parameters" Table (as December 2010) by Network, Stations, Dates, Number of Events, Magnitude range, Epicentral distance (selected data) and number of components

Network	#Stations	Dates	# Events	Magnitude	Epic. distance (km)	# Components
IST Azores	20	1996-2006	175	3.0 – 5.9	1 – 253	786
IST (S.P.)	17	1996-2006	23	3.1 – 5.5	2 – 490	180
IGC	11	1996-2008	23	3.0 – 5.2	8 – 240	147
ISTerre/RAP	88	1995-2007	387	3.0 – 6.8	1 – 863	5,232
KOERI	170	1998-2007	1160	3.0 – 7.4	1 – 653	6,522
ETHZ	29	2003-2009	80	3.0 – 5.3	0 – 200	1,902
ITSAK	39	2003-2008	398	3.0 – 6.9	2 – 496	1,871
IGN	82	1993-2010	276	3.0 – 6.2	1 – 652	2,226
ITDPC	91	1998-2004	107	3.0 – 5.6	1 – 476	1,095
Total	547	1993-2010	2629	3.0 – 7.4	0 – 863	19,961

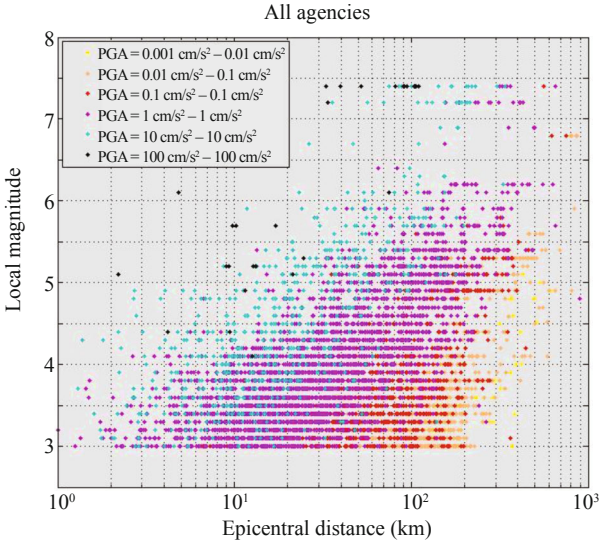

Fig. 2 Distribution of the arithmetic average of PGA of both horizontal components on a magnitude - distance plot

distance; finally, we analyze the dependence of soil conditions on accelerometric parameters.

3.1 Correlation between accelerometric parameters

Various authors have studied correlations between these engineering parameters, which were obtained from several strong motion data sets; however, these studies often have a limited number of samples (Aochi and Douglas, 2006; Baker and Jarayam, 2008; Bradley, 2010). In our case, we are dealing with a large database, which allows us to estimate the relation between the different parameters by analyzing the correlation between different pairs, either for each agency or for the entire dataset, including the dependence on magnitude and epicentral distance. Although these correlations have already been established, our analysis of this large European data set confirms, in many respects, the findings of other authors that are commonly used in engineering practice.

Table 3 presents the values of the linear correlations between the logarithms of the different above mentioned engineering parameters, for each agency′s data and for the entire data set. The following pairs of parameters have been selected for discussion:

(a) AI−PGA. Figure 3 illustrates a plot of the correlation between AI and PGA, in a log-log scale, for the entire data set and for different classes of magnitude.

The plot in Fig. 3 and the corresponding fitting results (Table 3) show a very good correlation coefficient (ρ = 0.98), which is equivalent to a standard deviation of the AI of a factor of 2 (σ (log AI) = 0.33).

The dispersion can be partially due to data from different agencies and with different magnitudes and distance ranges:

- Some small differences appear in the slope of each agency (Table 3).
- There is no difference in slope for different magnitudes (Fig. 3) and distances.
- Larger magnitudes (Fig. 3) or distances are related to higher AI values for the same PGA. Indeed, a factor of 10 is observed in the mean values of the AI when the magnitude increases from 3 to 6 or when the distance increases from 10 to 300 km (not shown).

Consequently, the AI is well correlated with PGA, but the last observation reflects the fact that we can have the same value of PGA for either a large magnitude event recorded at large distances or for a small magnitude event recorded at short distances. Obviously, the AI is greater for the first case, which is associated to a record with larger energy.

(b) CAV−PGA. The correlation coefficient for the entire data set is slightly smaller (ρ = 0.93) than that for AI−PGA. Similar observations can be made for the influence of agencies, magnitude and distance, and consequently, the parameter CAV also reflects the energy content of the record.

Table 3 Linear correlation parameters (a, b, and correlation coefficient, ρ) fitted to different engineering parameters pairs, in a log-log scale, for each agency data and for the entire data set (OverAll). For the entire data set, the standard deviation of the dependent variable is given

		ICGC	IST	ITSAK	KOERI	RAP	ETHZ	OverAll
$\log(AI) = a\cdot\log(PGA) + b \pm \varepsilon$	a	1.71	1.86	2.03	1.86	1.76	1.79	1.83
	b	-3.41	-2.96	-3.14	-2.97	-3.07	-2.85	-2.99
	ρ	0.92	0.94	0.95	0.94	0.98	0.95	0.98 (σ = 0.33)
$\log(CAV) = a\cdot\log(PGA) + b \pm \varepsilon$	a	0.71	0.81	0.99	0.84	0.75	0.84	0.82
	b	0.06	0.56	0.36	0.50	0.40	0.57	0.48
	ρ	0.74	0.84	0.86	0.83	0.92	0.91	0.93 (σ = 0.28)
$\log(CAV) = a\cdot\log(AI) + b \pm \varepsilon$	a	0.49	0.47	0.52	0.49	0.44	0.49	0.46
	b	1.71	1.91	1.97	1.92	1.78	2.00	1.86
	ρ	0.94	0.96	0.97	0.96	0.98	0.99	0.98 (σ = 0.15)
$\log(SA\ (39.07\ Hz)) = a\cdot\log(PGA) + b \pm \varepsilon$	a	1.06	0.95	0.88	1.00	1.03	1.28	0.95
	b	0.17	-0.03	0.01	-0.21	0.01	0.03	-0.09
	ρ	0.95	0.96	0.97	0.94	0.97	0.46	0.97 (σ = 0.19)
$\log(PSV_{max}) = a\cdot\log(PGV) + b \pm \varepsilon$	a	1.01	1.02	0.96	0.96	1.02	1.16	0.99
	b	0.45	0.46	0.33	0.42	0.47	0.73	0.43
	ρ	0.98	0.96	0.97	0.98	0.98	0.91	0.99 (σ = 0.13)
$\log(PGA/PGV) = a\cdot\log(\text{freq. } PSV_{max}) + b \pm \varepsilon$	a	0.64	0.57	0.70	0.71	0.74	0.57	0.70
	b	1.21	1.10	1.03	1.05	1.06	1.39	1.05
	ρ	0.85	0.77	0.78	0.86	0.86	0.69	0.85 (σ = 0.16)
$\log(PGA/PGV) = a\cdot\log(TD) + b \pm \varepsilon$	a	-0.33	-0.22	-0.53	-0.51	-0.53	0.04	-0.36
	b	2.09	1.71	2.05	2.00	2.30	1.62	1.87
	ρ	-0.52	-0.32	-0.57	-0.57	-0.60	0.02	-0.44 (σ = 0.27)
$\log(CAV) = a\cdot\log(HI) + b \pm \varepsilon$	a	0.69	0.72	0.86	0.71	0.78	0.65	0.73
	b	1.39	1.50	1.45	1.36	1.53	1.40	1.37
	ρ	0.87	0.90	0.92	0.91	0.87	0.59	0.94 (σ = 0.25)
$\log(AI) = a\cdot\log(HI) + b \pm \varepsilon$	a	1.26	1.48	1.59	1.39	1.71	1.42	1.55
	b	-0.94	-0.93	-1.01	-1.19	-0.72	-0.98	-1.09
	ρ	0.83	0.91	0.92	0.91	0.86	0.63	0.94 (σ = 0.54)

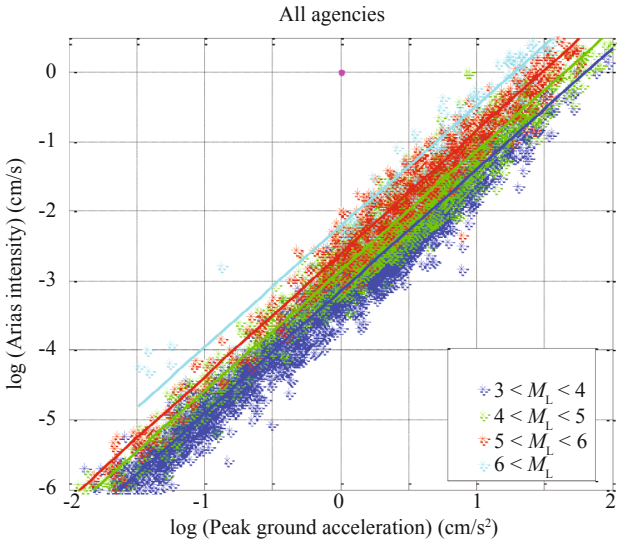

Fig. 3 Correlation between AI-PGA for the entire data set, for different classes of magnitude

(c) CAV-AI, CAV-HI and AI-HI. For all these pairs, the data show a very good correlation coefficient (ρ > 0.94). No significant differences are observed for individual agencies (Table 3) or for magnitudes and distances. Therefore, a high statistical dependence appears to exist between CAV, AI and HI, as expected based on their definitions.

(d) PSA (39 Hz)−PGA. This correlation is made to compare the asymptotic behavior of the response spectrum at a high frequency, represented by PSA (39 Hz), and the PGA. The fit show a good correlation (ρ = 0.98) and coincidence between these two parameters.

These results confirm two evidences: (i) new digital instrumentation are reliable at high frequencies (50 Hz), and, consequently, there is no need for low-pass filtering, in agreement with our procedure; and (ii) the results from a recent study by Bommer *et al.* (2012) indicate the insensitivity of high-frequency spectral ordinates to record processing in high frequencies.

(e) PSV_{max}−PGV. This correlation is made to compare the maximum value of the pseudo-velocity response spectrum with the PGV. The correlation is very good (ρ = 0.98). No differences are observed for individual agencies (Table 3) or for variations in magnitude and distance. The value of the *b*-coefficient, 0.43 (Table 3), is equivalent to a factor of 2.7 for the linear ratio between PSV_{max} and PGV. This factor is slightly greater than that for the well-known Newmark design spectra, 1.9 (Newmark and Hall, 1982; Naeim, 2001). In a recent study, Booth (2007) proposed a mean value of 2.3.

Summarizing the obtained results, we can emphasize the following aspects:

- PGA is well correlated with CAV, AI and HI, but the correlation coefficients are strongly dependent on the magnitude and the epicentral distance.
- CAV, AI and HI are well correlated with each other because these values are indicators of the energy content.
- As expected, the asymptotic behavior of the response spectrum at high frequencies, represented by PSA (39 Hz), shows a very good correlation with PGA, clearly indicating the high-frequency response of digital stations.
- PGV is highly correlated with PSV_{max}, with the *b*-coefficient slightly larger than the values previously published.

3.2 Dependence of PGA horizontal components on magnitude and epicentral distance

The data set contained in the "Event,...,Parameters" Table is of great interest to compare weak and moderate motion records from different agencies, as illustrated in Fig. 4, where the PGA values from RAP and ITSAK events, with magnitudes between 4 and 5, are plotted versus epicentral distance. Note the consistency between PGA data of these two agencies. Also, the recording threshold of the instruments from ITSAK is much higher than that from RAP, and merging data from the two agencies presents a more complete view of the entire attenuation phenomenon. Additionally, all data show larger inter-station and intra-event scatters, but not much inter-agency scatter, as described above.

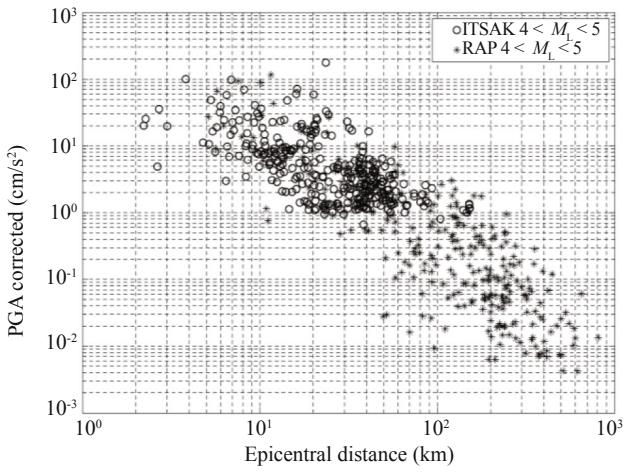

Fig. 4 Average PGA values for horizontal components corresponding to a range of magnitudes between 4 and 5, recorded by RAP and ITSAK plotted versus epicentral distance

Figure 5 ((a), (b), (c) and (d)) presents the arithmetic average of PGA values for horizontal components versus epicentral distances, of all agencies grouped by intervals of magnitude: *M*3–4 (4,321); *M*4–5 (1,575); *M*5–6 (633); and *M* > 6 (149). The figure in parentheses represents the number of records.

A first measure of the large scatter of the data is made using box-plot diagrams for the following distance bins, which are equally spaced logarithmically: 1−10 km, 10−20 km, 20–40 km, 40−100 km, 100−200 km, 200–400 km and 400−1000 km; similar measurements were made for the 4 magnitude ranges. The box-plot diagram represents a summary with five numbers: the smallest observation (sample minimum), the lower quartile (Q1), the median (Q2), the upper quartile (Q3) and the largest observation (sample maximum). Q1 and Q3 exclude the lowest 25% and 75% of corresponding data, respectively, to the 25th and 75th percentile. Herein, we define Y_{min} = Q1 – 1.5 × (Q3 – Q1) and Y_{max} = Q3 + 1.5 × (Q3 – Q1). The box diagram may also indicate which observations, if any, might be considered "outliers" (< Y_{min} or > Y_{max}).

These displays emphasize only the differences between populations without making any assumptions of underlined distributions.

Figure 5 reveals that the general dispersion of data points is quite large specially for lower magnitudes ranges of the order of a factor of 10^2. In the following section, we analyze the box diagrams of data points for each magnitude range:

(a) For *M*3–4 (Fig. 5(a)):

- For the Q3−Q1 interval, representing 50% of the data belonging to the distance bin, Q3/Q1 = 3 for epicentral distances < 50 km. For distances 50−100 km, Q3/Q1 > 10. For distances > 100 km, the ratio Q3/Q1 decreases.
- For distance bins with more than 100 data points, the boxes show a symmetric distribution, except for distances > 100 km, where Y_{max} – Q3 is greater than Q1 – Y_{min} and where some "outliers" are greater than Y_{max}

(b) For M4–5 (Fig. 5(b)):

- For the Q3−Q1 interval, Q3/Q1 = 3 for epicentral distances < 100 km. For distances > 100 km, Q3/Q1 = 10.
- For distance bins with more than 100 data points, the boxes show a symmetric distribution, except for distances > 100 km, where Y_{max} – Q3 is lesser than Q1 – Y_{min}, which is contrary to the observation for the same distance bin for *M*3–4.

(c) For M5–6 (Fig. 5(c)):

- For the Q3 – Q1 interval, Q3/Q1 = 3 for epicentral distances < 200 km. For distances > 200 km, Q3/Q1 = 10.

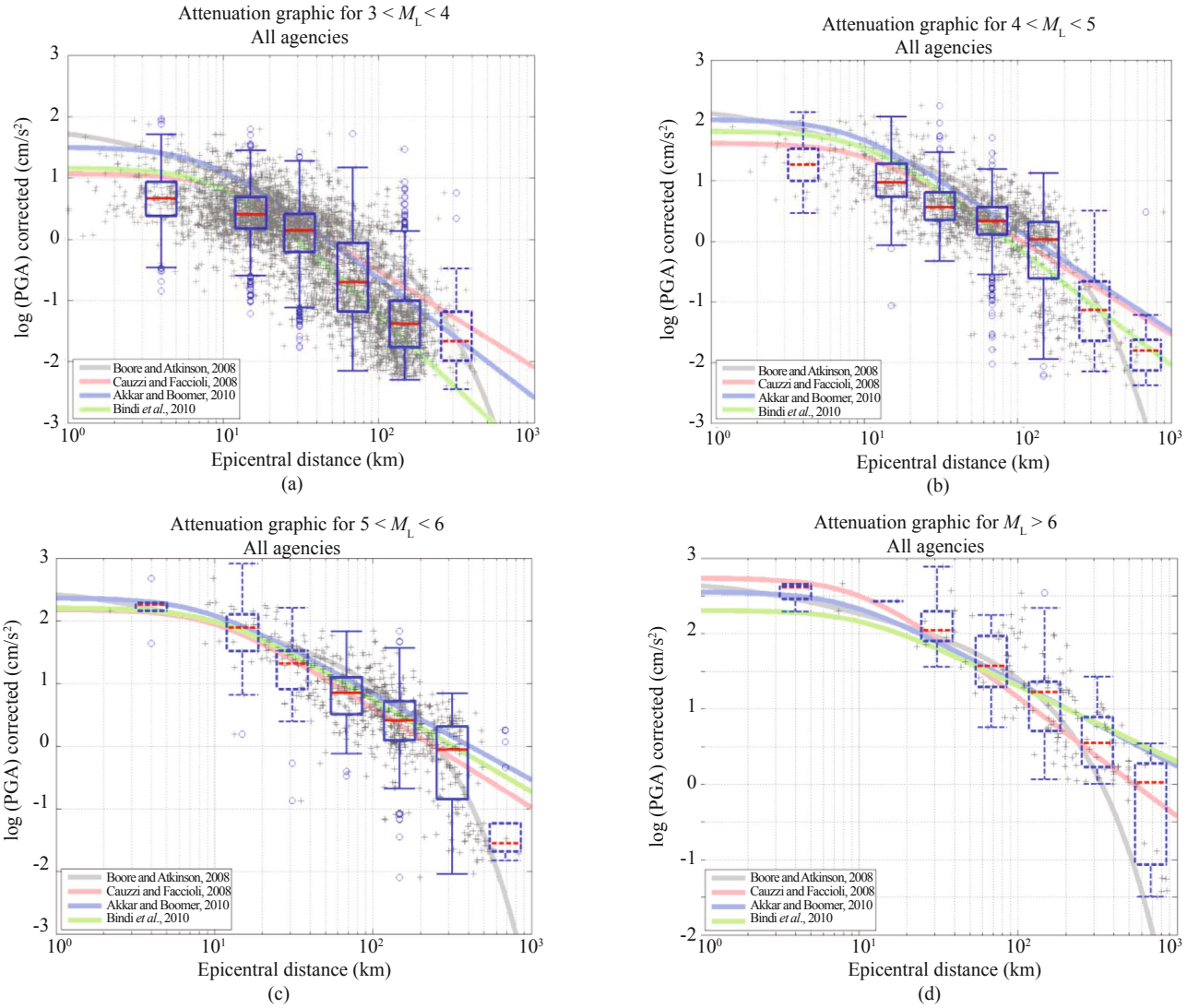

Fig. 5 Average PGA values for horizontal components versus epicentral distances of all agencies grouped by intervals of magnitudes: *M*3–4; *M*4–5; *M*5–6 and *M* > 6. Box values (Q1-blue, Q2-red, Q3-blue) for different epicentral distances are also plotted. The circles represent outliers, which are data points outside the interval (Y_{min}–Y_{max}), represented by horizontal blue bars. The dashed representation is made for the case of less than 100 data points. Mean values of four GMPE are included, for each magnitude interval average: Boore and Atkinson (2008), Cauzzi and Faccioli (2008), Akkar and Bommer (2010) and Bindi *et al*. (2010)

- For distance bins with more than 100 data points, the boxes show a symmetric distribution, except for distances > 200 km, where Y_{max} – Q3 is lesser than Q1 – Y_{min}, similarly to the observation for the same distance bin for *M*4-5.

(d) For *M* > 6 (Fig. 5(d)): because all distance bins have less than 100 data points, the tendencies are not representative.

The definition of distance as the epicentral distance is adequate for this data set because most of the events have *M* < 6, for which no significant extension of fault ruptures is observed. Only 446 records from 17 events with *M* > 6 could be affected by this definition.

The possible sources of the observed dispersion are described below:

- The first source is inherent to the classification of data by bins of one degree of magnitude. Differences in the magnitude assignment performed by each agency are also a source of uncertainty, even though the majority of the magnitude values in this database are M_L.
- Possible regional tectonic settings, often argued as a possible source of differences in the attenuation tendencies (Douglas, 2011), might be another source of uncertainty. However, as we have shown in Fig. 4, no significant differences were observed for the whole set of data points for two agencies with different tectonic environment. The same visual comparison was performed for all other agencies, leading to similar conclusions.
- Dispersion due to the soil conditions of different recording stations. This will be analyzed in the next section.

To complete this analysis, we refer to a recently published study (Delavaud *et al.*, 2012), whose objective

was to choose a ground motion logic tree for PSHA (Probabilistic Seismic Hazard Assessment) in Europe. Toward this end, the authors proposed a methodology combining "expert judgment" and "data-test results" to select the most appropriate option among an important number of existing GMPEs (Ground-Motion Prediction Equations) derived for different tectonic environments. In this context, we can consider that the so-called ASCRs (Active Shallow Crustal Regions) contain the areas where most of our database is compiled (see Figs. 1(a), (b)). Delavaud *et al.* (2012), following the "data-test results", used two databases (DB1, DB2). DB1 is composed of 1533 records from Europe, mainly from Turkey, for magnitude and distance ranges of $4 < M_w < 7$ and 1 km < RJB < 200 km, obtained the following ranking of the candidate GMPEs adapted to short periods ($T < 3.0$ s): Bindi *et al.* (2010), Cauzzi and Faccioli (2008) and Cotton *et al.* (2008). Due to the lack of large magnitude events in DB1, GMPEs were also tested against DB2, which is mainly composed of 1755 non-European recordings of magnitudes between 6 and 8, yielding the following ranking of the candidate GMPEs adapted to short periods ($T < 3.0$ s): Akkar and Bommer (2010), Chiou and Youngs (2008) and Boore and Atkinson (2008).

In Fig. 5, we also plotted four of the above mentioned GMPEs: Bindi *et al.* (2010), Cauzzi and Faccioli (2008), Akkar and Bommer (2010) and Boore and Atkinson (2008). The mean values of the four GMPEs are included for each magnitude interval average.

In the following section, we discuss briefly the adaptation of the four above mentioned GMPEs to the present data:

- For distance bins between 10 km and 200 km, for which box-plots are well defined, especially for $M < 6$, the 4 selected GMPEs fit the central percentiles Q1(25%), Q2(50%) and Q3(75%) of data quite well;
- For distance bins of 1−10 km and for $M < 5$, for which the sample size of the data seems representative, all of the GMPEs overestimate the data, with Bindi *et al.* (2010) and Cauzzi and Faccioli (2008) being the best adapted to the data;
- For distances greater than 200 km, even if the sample data are not well represented, Boore and Atkinson (2008) seem to take into account the high attenuation shown by data, in particular for *M*5–6.

Consequently, the present data, combining both small and large magnitude events and epicentral distances, and thus leading to a mixture of weak and moderate ground motions, represent a powerful database to improve studies on how to choose GMPEs that are well adapted to the Euro-Mediterranean area (Delavaud *et al.*, 2012).

3.3 Soil dependence of the accelerometric parameters

To study the soil influence on the ground motion parameters as a function of magnitude and epicentral distance for all data, we first selected three parameters: PGA, which represents the high-frequency content; PGV, which represents the medium-frequency content; and HI, which represents the overall frequencies content. Then, we analyzed all spectral shapes similarly using PSV (*f*) for 28 frequencies.

3.3.1 PGA, PGV and HI analysis

First, we used a soil classification of R, H or S. Approximately 33% of the records are classified as R, whereas 46% and 21% of the records are classified as H and S, respectively.

We have considered the average PGA, PGV and HI values for the horizontal components multiplied by the epicentral distance. Such distance normalization is supported by the attenuation relationships that are generally proportional to the distance (DEpi) elevated to an exponent close to (−1) (Rey *et al.*, 2002). This analysis has been presented in detail in Goula *et al.* (2012).

Figure 6 illustrates the data points PGA×DEpi normalized by the mean value of the distances in each bin, for the range of magnitudes *M*4–5 and for the following distance bins, equally spaced logarithmically: 1−10 km, 10−20 km, 20−50 km, 50−100 km, 100−200 km and > 200 km. For each range of magnitudes, the mean value and the standard deviation in each distance bin for each R, H, and S soil class were also computed.

This plot shows that R sites always present lower values than H and S sites, clearly indicating that H and S sites amplify ground motion (PGA) compared with R sites. The same observation applies to PGV and HI. Because there is no clear differentiation between H and S sites (Fig. 6), we have similarly analyzed the data recorded in stations with available EC8 soil classifications of A, B, C, D and E (EC8, 2004) (ITDPC, KOERI, IGN and RAP), corresponding to approximately 60% of the total available data.

We confirmed the same pattern of no differentiation

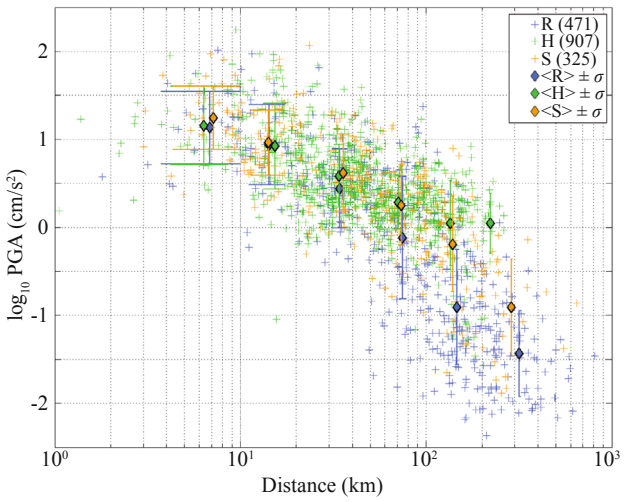

Fig. 6 Average of PGA values for horizontal components multiplied by epicentral distance and normalized by the mean value of distances in each bin versus epicentral distances for the interval *M*4–5 with different soil classification (R, H and S) done by each agency. Mean value and standard deviation for $\log_{10}$(PGA) data in each bin, for each soil class, are also shown

between H and S for all other parameters, described in Section 3.1: PGA, PGV, AI, TD, CAV and HI, together with PSV (*f*) for 28 frequencies. The figures with the plotted data (not shown) are similar to Fig. 6.

Figure 7 shows the ratios between the mean values of PGA, PGV and HI, of the Soil Classes B and C in relation to A (B/A and C/A) per magnitude class and distance bin. The ratios are interpreted as indicators of soil amplification and were computed from average values over magnitude classes and distance bins, considering a minimum of 10 points in each magnitude and distance class. The data for D and E classes are not in sufficient number to be analyzed with statistical meaning.

We observe a strong influence of distance on the ratios, i.e., the amplification is almost inexistent for short distances but increases for larger distances. An important influence of magnitude was also observed. In all figures, greater ratios are obtained for the small magnitude range (*M*3−4 data).

This influence of distance and magnitude on soil amplification ratios seems to indicate that weak motion, corresponding to low magnitudes and larger distances, shows larger amplification than strong motion recorded at short distances for large magnitudes. Therefore, to interpret ratios as indicators of soil amplification, we will retain only ratios for distances less than 200 km and for $M < 6$, because the data for this range of distances and magnitudes are better represented.

If, for engineering purposes, we further restrict our analysis to a range of distances of 0−100 km and a range of magnitudes *M*4–6, which produce significant ground motion in the Euro-Mediterranean region, the amplification values become smaller, with less variability. These results, presented in Table 4, can be compared with the soil coefficient *S* for the Type 2 EC8 response spectra, which is in the framework of our data set.

A clear large dependence on distance is observed for different amplification values. Although the *S*-coefficient of EC8 is similar to the PGA amplification for short distances, these values are much larger for greater distances. Moreover, the PGV amplification values are large, indicating the influence of spectral shapes (see next section). These differences are even larger for HI amplification values, because the HI represents

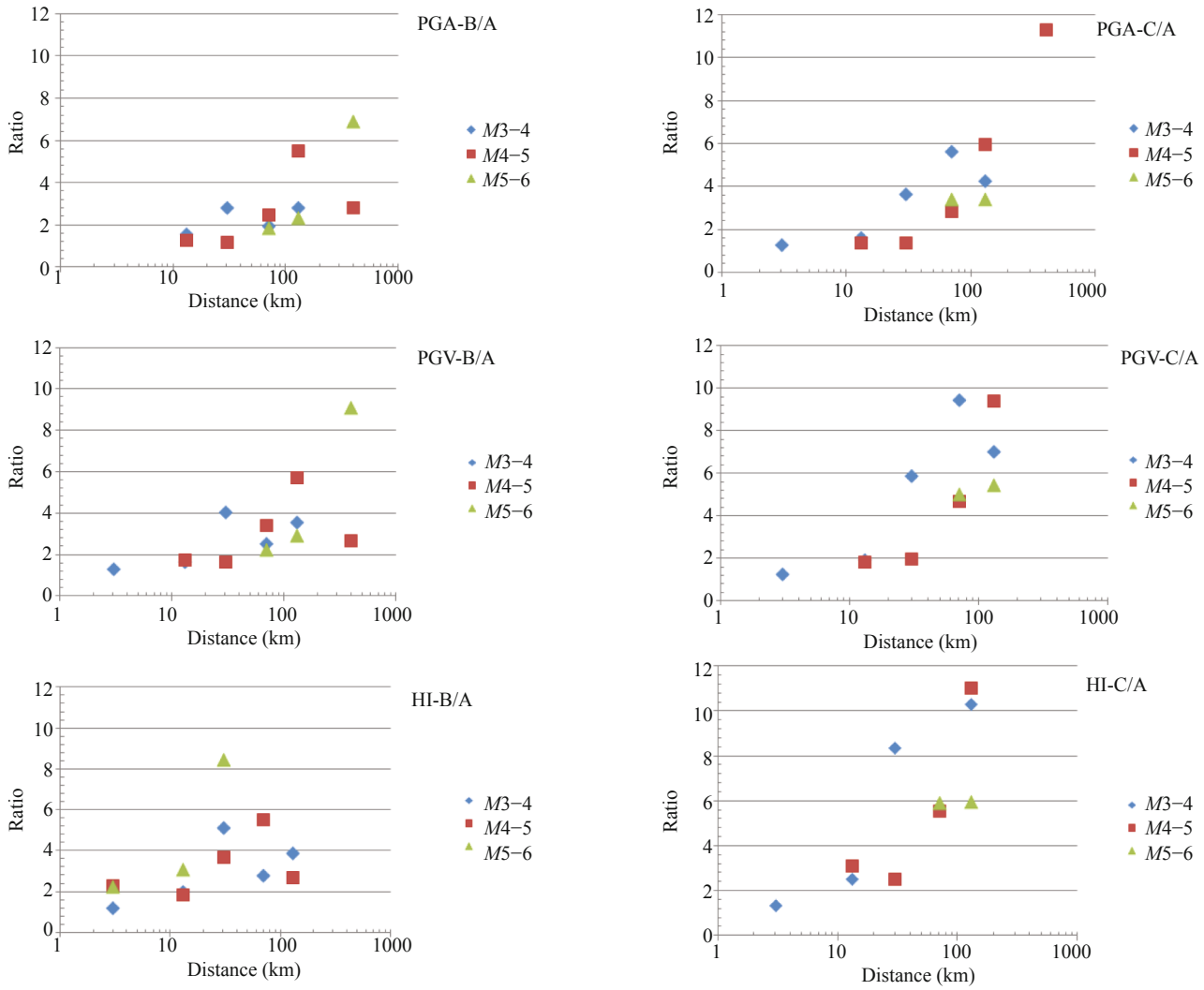

Fig. 7 Ratios between mean values of PGA, PGV and HI of different EC8 soil Classes (B and C) and A (B/A and C/A), per magnitude classes and distance bins

Table 4 Average ratio values between EC8 soil classes B/A and C/A for PGA, PGV and HI parameters for 2 ranges of distances, for *M*4–6, compared to soil coefficient *S* for Type 2 EC8 response spectra and UBC97 amplification coefficients (Rodriguez-Marek *et al.*, 1999)

	Short dist			Long dist			EC8 Type 2	UBC97	
	PGA	PGV	HI	PGA	PGV	HI	*S*-coeff	F_a	F_v
B/A	1.27	1.76	2.29	1.86	2.41	2.51	1.3	1.0–1.2	1.4–1.7
C/A	1.37	1.86	3.12	2.78	4.18	4.98	1.5	1.1–1.6	1.6–2.4

the entire spectral content (Rey *et al.*, 2002). Similar amplification factors due to ground motion level and frequency content are also considered in UBC97 of the USA (Rodriguez-Marek *et al.*, 1999), as shown in Table 4, where F_a and F_v, respectively, are considered short-period and mid-period spectral amplification factors. In fact, soil equivalence can be assumed between the UBC97 and EC8 soil classifications if A, B and C soil types for EC8 are considered B, C, and D soil types for UBC97 classes. The range of values shown in Table 4 for UBC97 corresponds to a range of PGA between 0.4 g (strong ground motion) and 0.08 g (weak motion) (Rodriguez-Marek *et al.*, 1999).

The tendencies shown in the European data are the same as those in UBC97; however, the range of input levels is lower for long distances, and consequently, the factors are higher.

3.3.2 Spectral analysis

We will analyze the influence of soil conditions on all of the spectral values (28 frequencies) for different ranges of magnitudes and distances, comparing the PSA values (5%) to different soil conditions of EC8 (2004) spectral forms. To analyze the "spectral forms", we compute each record PSA(f) = $2\pi f \times$PSV(f) and normalize all values to their PGA.

The EC8 soil classes A, B and C were used to analyze the normalized spectral values of PSA(f)/PGA. For all the available data, we computed the *mean value* and the *standard deviation* for each frequency of the normalized values for the different soil classes.

Figure 8 shows, for all agencies, the *mean value* of the normalized spectrum (in relation to PGA) for the three classes of soil for the *M*3–4, *M*4–5 and *M*5–6 ranges and three classes of distance: 0−20 km, 20−100 km and 100−200 km. For $M > 6$ and $D > 200$ km, data are not sufficient to pursue the analysis. Type 1 and Type 2 EC8 response spectral shapes are also shown for the soil classes A, B and C (with the design soil coefficient S assigned to 1).

In fact, very few differences exist in EC8 for the values of T_b and T_c, which define the spectral form for Type 2 (T_b = 0.05 s for Classes A and B and 0.10 s for class C; T_c = 0.25 s for the three classes). For Type 1, these differences are larger: T_c = 0.4, 0.5 and 0.6 s for the Classes A, B and C, respectively. Thus, the soil amplification proposed in EC8 Type 2 is essentially represented by the Design Soil Coefficient S, and not by the spectral form.

The following observations can be made from Fig. 8:

- The uncertainties shown on all normalized spectral values are partially due to the bin range of one degree of magnitude and to the bin range of distances considered.
- These uncertainties are clearly larger than the differences between the average spectral values shown for different soil classes.
- The average spectral shapes show a consistent tendency of larger differentiation of the Soils A, B and C with increasing distances and increasing magnitudes.
- For Class A (rock sites), the mean spectral shapes show a "plateau" less than 2.5 for almost all cases. For Classes B and C, the "plateau" is near 2.5 in all cases.
- For *M*3–4, the spectral shapes are clearly below the Type 2 spectral shape, especially for distances less than 100 km. For the shortest distances, all 3 soil shapes are similar, whereas for distances greater than 20 km important differences are observed between soils C, B and A. This observation agrees with the previous results found with the PGA, PGV and HI analyses, where amplifications are larger for PGV and HI than for PGA (Fig. 7).
- For *M*4–5, the Type 2 spectral shape is better adapted to the average spectral shapes, even though important differences are observed between the C, B and A spectral shapes. This observation agrees with the previous results found with the PGA, PGV and HI analyses, where amplifications are larger for PGV and HI than for PGA (Fig. 7).
- For *M*5–6, no analysis is made for the shortest distances because of insufficient data. For distances between 20 and 100 km, the spectral shapes of Classes A and B are well adapted to the Type 2 shape, but for Class C, a clear amplification is shown. For distances greater than 100 km, the spectral shapes for Classes A, B and C show values between the Type 1 and Type 2 EC8 spectral shapes. Differences between soil classes are very similar to those proposed for Type 1 shapes.

As in the previous section, if we restrict our analysis to a range of distances of 0−100 km and to a range of magnitudes of *M*4–6, for engineering purposes, the main significant result is that the average spectral shapes are well adapted to the Type 2 EC8 shape, but the differences observed between the C, B and A soil classes agree with the larger amplification of PGV and HI parameters than that of PGA for the C and B classes.

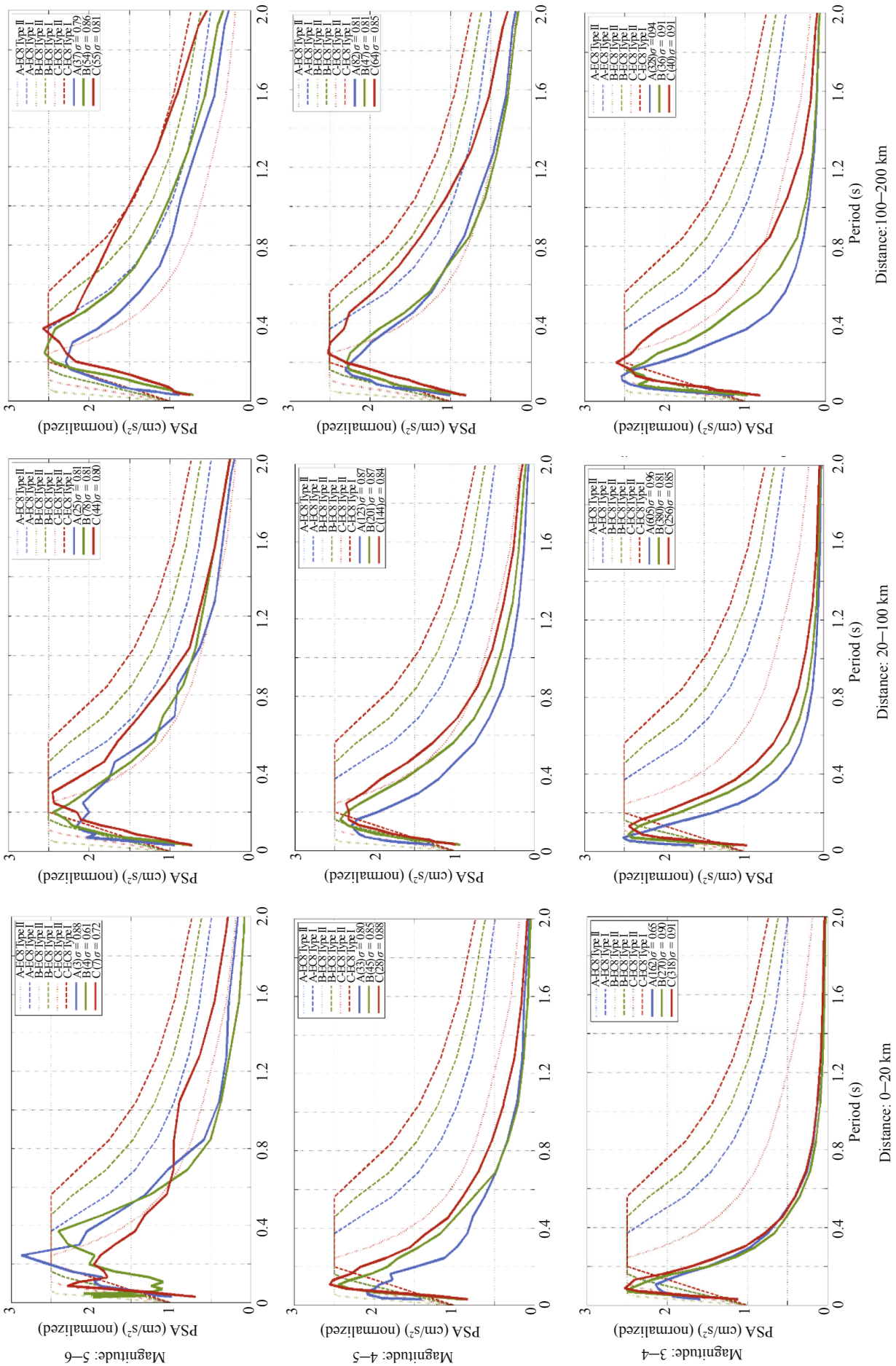

Fig. 8 Average normalized response spectra for records on EC8 Soil Classes A, B and C, for three magnitude and three distances ranges. The number of components analysed and the standard deviation are indicated in the upper part of the figures. EC8 Type 1 and 2 for Soils A, B and C classes are also plotted ($S = 1$)

4 Conclusions

In this paper, we present an overall analysis of ground motion parameters (PGA, AI, TD, CAV, PGV and HI, together with PSV(*f*,5%) for 28 frequencies) determined from a large set of digital accelerograms recorded in Europe from 1993 to December 2010 by eight different agencies; these parameters were computed in a homogeneous manner with a standard procedure.

The total number of stations recording 2,629 events with $3.0 < M < 7.4$ was 547, approximately half of which are classified as "rock sites–R", whereas the other half are classified as a mixture of "hard–H, and soil–S sites". A total of 19,961 individual components were used. For approximately 60% of these data, a more refined classification of soils based on EC8 classes (A to E) exists.

To estimate the relation between the different parameters, we calculated the correlations between different pairs, either for each agency or for the entire data set, including the dependence of parameters on magnitude and epicentral distance. Even though the results follow similar trends as observed in previous worldwide datasets, there are a few differences, such as the magnitude dependence.

The analysis of PGA versus epicentral distance was performed based on 4 classes of magnitude, *M*3–4, *M*4–5, *M*5–6 and $M > 6$, using box diagrams for various distance bins. The possible sources of large dispersion were also analyzed, and four recent GMPEs which were selected as the best adapted to the Euro-Mediterranean region by Delavaud *et al.* (2012) were included. It was concluded that these GMPEs are well adapted to the present data in the epicentral distances range $10 < R <$ 200 km. However, for very short (< 10 km) and very long distances (> 200 km), the present data seem to indicate a different behavior than that predicted by the GMPE selected by Delavaud *et al.* (2012). Consequently, the present data, combining both low and large magnitude events as well as small and large epicentral distances, represent a powerful database to improve studies on how to choose GMPEs that will be better adapted to the Euro-Mediterranean area.

In relation to soil conditions, we found that the simple soil classification used for all stations (R, H and S) is not sufficiently precise to quantify the soil influence on several parameters that were analyzed (PGA, PGV, HI and PSV (*f*)). However, analysis using the EC8 Soil Classes A, B and C, when available, showed a clear soil dependence on magnitude and epicentral distance.

Soil amplification ratios indicate that weak motion (low magnitudes and larger distances) shows larger amplification than strong motion (short distances and large magnitudes) as represented in UBC97 (1997) for the USA, but not represented in EC8 (2004) for Europe.

For engineering purposes (i.e., *M*4–6 and distances of 0−100 km), we made the following observations:

- The PGA amplification for short distances is similar to the *S*-coefficient of EC8, whereas for larger distances, these values are much larger.

- The PGV amplification values show larger values, indicating the influence of spectral shapes.

- These differences are even larger for HI amplification values, as the HI represents the entire spectral content.

- The average spectral shapes are well adapted to the Type 2 EC8 shape, but differences were observed between the C, B and A classes, in agreement with previous observations.

- For Class A (rock sites), the mean spectral shapes showed a "plateau" less than 2.5 for almost all cases. For Classes B and C, the "plateau" was near 2.5 in all cases.

Similar observations were found by Pitilakis *et al.* (2012), who analyzed a global data set. The average normalized spectral forms were found to be less than the EC8 proposed forms for intermediate and long periods. Additionally, amplification factors were found to be frequency dependent; however, the authors concluded that it is not necessary to improve spectral forms and that only an independent soil amplification factor (*S*) is prone to be enlarged for all soil classes.

Our results could be incorporated into a Type 2 EC8 spectra revision, reducing the 2.5 factor for the "plateau" for Class A and keeping the 2.5 factor for Classes B and C. In this manner, observations concerning both the spectral shapes and the frequency dependence of amplification factors could be considered.

The analyses and interpretations made in this study constitute an initial contribution to improved characterization of the digital accelerometric data that are recorded in the European region. The material presented in this paper has great potential for further development.

Acknowledgement

This paper has been partially supported by the EC Project NERIES, Sixth Framework Programe, Contract number: RII3-CT-2006-026130. Special thanks are due to all of the authors′ institutions for financial support. The authors would like to acknowledge all of the networks that made available their data, including the French RAP (Réseau Accelerometrique Permanent), represented by ISTerre, and their representatives: C. Zulfikar (KOERI), C. Papaioannou (ITSAK), P. Guéguen (ISTerre), J. Clinton (ETHZ), L. Luzi (ITDPC), L. Cabañas (IGN) and S. Godey (EMSC). Jordi Roviró is acknowledged for contributions to the soil analyses. Special thanks are due to Antoni Roca for project coordination and support. We also acknowledge Gail Atkinson for her support during the preparation of the manuscript and Isabel Viseu for helping to review the final version of the text.

References

Akkar S and Bommer J (2006), "Influence of Long-period Filter Cut-off on Elastic Spectral Displacements," *Earthquake Engineering and Structural Dynamics*,

35:1145–1165.

Akkar S and Bommer J (2010), "Empirical Equations for the Prediction of PGA, PGV and Spectral Accelerations in Europe, the Mediterranean Region and the Middle East," *Seismological Research Letters*, **81**:195–206.

Ambraseys NN, Smit P, Douglas J, Margaris B, Sigbjörnsson R, Ólafson S, Suhadolc P and Costa G (2004), "Internet Site for European Strong Motion Data," *Bolletino di Geofisica Teorica ed Applicata*, **45**: 113–129.

Aochi H and Douglas J (2006), "Testing the Validity of Simulated Strong Ground Motion from the Dynamic Rupture of a Finite Fault, by Using Empirical Equations," *Bulletin of Earthquake Engineering*, **4**: 211–229.

Archuleta RJ, Steidl J and Squibb M, (2006), "The COSMOS Virtual Data Center: a Web Portal for Strong Motion Data Dissemination," *Seismological Research Letters*, **77**(6):651–658.

Arias A (1970), "A Measure of Earthquake Intensity," in RJ Hansen (editor), *Seismic Design for Nuclear Power Plants*, MIT Press, Cambridge, MA, 438–483.

Atkinson GM (2012), "Integrating Advances in Ground-motion and Seismic-hazard Analysis," Key-note lecture, *Proceedings 15 World Conference on Earthquake Engineering*, Lisbon, Portugal.

Baker J and Jarayam N (2008), "Correlation of Spectral Acceleration Values from NGA Ground Motion," *Earthquake Spectra*, **24**: 299–317.

Bindi D, Luzi L, Massa M and Pacor F (2010), "Horizontal and Vertical Ground Motion Prediction Equations Derived from the Italian Accelerometric Archive (ITACA)," *Bulletin of Earthquake Engineering*, **8:** 1209–1230.

Bommer J, Akkar S and Drouet S (2012), "Extending Ground Motion Prediction Equations for Spectral Accelerations to Higher Response Frequencies," *Bulletin of Earthquake Engineering*, **10**(2): 379–399.

Boore D and Akkar S (2003), "Effect of Causal and Acausal Filters on Elastic and Inelastic Response Spectra," *Earthquake Engineering and Structural Dynamics*, **33**: 1729–1748.

Boore DM and Atkinson GM (2008), "Ground Motion Prediction Equations for the Average Horizontal Component of PGA, PGV and 5%-Damped PSA at Spectral Periods between 0.01 s and 10.0 s," *Earthquake Spectra*, **24:** 99–138.

Booth E (2007), "The Estimation of Peak Ground-Motion Parameters from Spectral Ordinates," *Journal of Earthquake Engineering*, **11**(1):13–32.

Bradley B (2010), "Correlation of Significant Duration with Amplitude and Cumulative Intensity Measures and Its Use in Ground Motion Selection," *Journal of Earthquake Engineering*, **15**: 809–832.

Cabañas L, Benito B and Herráiz M (1997), "An Approach to the Measurement of the Potential Structural Damage of Earthquake Ground Motion," *Earthquake Engineering and Structural Dynamics*, **26**:79–92.

Çagnan Z, Akkar S and Gülkan P (2011), "A Predictive Ground-motion Model for Turkey and Its Comparisons with Recent Local and Global GMPE´s," in: S Akkar, P Gülkan, T Van Eck (editors), *Earthquake Data in Engineering Seismology: Metworks Data Management and Predictive Models*, Geotechnical, Geological and Earthquake Engineering Book Series, Chapter 4, Springer, 39–53.

Cauzzi C and Faccioli E (2008), "Broad Band (0.05 to 20 s) Prediction of Displacement Response Spectra Based on Worldwide Digital Records," *Journal of Seismology*, **12**:139–171.

Chiou BS and Youngs RR (2008), "An NGA Model for the Average Horizontal Component of Peak Ground Motion and Response Spectra," *Earthquake Spectra*, **24**:174–215.

Cotton F, Pousse G, Bonilla F and Scherbaum F (2008), "On Discrepancy of Recent European Ground-motion Observations and Predictions from Empirical Models: Analysis of Kik-Net Accelerometric Data and Point-sources Stochastic Simulations," *Bulletin of the Seismological Society of America*, **98**: 2244–2261.

Delavaud E, Cotton F, Akkar S, Scherbaum, Danciu L, Beauval C, Drouet S, Douglas J, Basili R, Sandikkaya MA, Segou M, Faccioli E and Theodoulidis N (2012), "Toward a Ground-motion Logic Tree for Probabilistic Seismic Hazard Assessment in Europe," *Journal of Seismology*, **16**(3):451–473.

Douglas J (2011), "Investigating Possible Regional Dependence in Strong Ground Motion," in: S Akkar, P Gülkan and T Van Eck (editors), *Earthquake Data in Engineering Seismology: Networks Data Management and Predictive Models*, Geotechnical, Geological and Earthquake Engineering Book Series, Chapter 3, Springer, 29–38.

Douglas J, Guéguen P, Chaljub E, Cotton F, Suhadolc P, Costa G, Faeh D, Spühler E, Gosar A, Priolo E, Barnaba C, Paolucci R, Cauzzi C and Eva C (2006), "Alpine Accelerometric Data-base," CDRom.

Earthquake Data Portal (2011), http://www.seismicportal.eu. (Accessed March 2011).

EC8 (2004), "Eurocode 8, Design of Structures for Earthquake Resistance, General Rules, Seismic Actions and Rules for Buildings," BS EN **1998–1**: 2004.

EMSC-CSEM (2011-2013), Euro-Mediterranean Seismological Centre: http://www.emsc-csem.org (Accessed in Feb 2013).

ESD (2013), "Internet Site for European Strong-Motion Database," http://www.isesd.hi.is/ESD (Accessed in Feb 2013).

Gassol G (2011), "Anàlisi i Validació dels Parameters d′accelerogrames de la Base de Dades Europea (NERIES Distributed Database) Calculats Homogèniament,"

Master Thesis, Universitat Politècnica de Catalunya, 372. (in Catalan)

Godey S (2010), Personal Communication.

Goula X, Susagna T, Oliveira CS and Roviró J (2012), "Soil Amplification Based on Statistical Analysis of NERIES European Digital Accelerometric Data-base," *Proceedings of 15th World Conference on Earthquake Engineering*, Lisbon, Portugal, September 24–28, 3996.

Housner GW (1952), "Spectrum Intensities of Strong-motion Earthquakes," *Proceedings of Symposium on Earthquake and Blast Effects on Structures*, Earthquake Engineering Research Institute, Berkeley, CA.

Husid R (1973), *Terremotos: Análisis Spectral y Características de Acelerogramas como base de Diseño Sí*smico, Andres Bello, 447. (in Spanish)

IGN (1999), Base de datos de aceleración 1984–1997, CR-Rom (in Spanish)

IGN (2010), Personal Communication.

ITACA (2010), http://itaca.mi.ingv-it/ItacaNet (Accessed Oct 2011).

Kinoshita S (2003), "Kyoshin Net (K-Net), Japan," Lee W, Kanamori H, Jennings P, Kisslinger C (editors) *International Handbook of Earthquake and Engineering Seismology*, Academic Press, International Association of Seismology and Physics of the Earth′s Interior, 1049–1056.

Kramer SL (1996), *Geotechnical Earthquake Engineering*, Prentice Hall Inc, Upper Saddle River, NJ, 651.

Lee W, Kanamori H, Jennings P and Kisslinger C (2002), *International Handbook of Earthquake and Engineering Seismology*, Academic Press, International Association of Seismology and Physics of the Earth′s Interior, 1942.

Luzi L, Hailemikael S, Bindi D, Pacor F, Mele F and Sabetta F (2008), "ITACA (Italian Accelerometric Archive): a Web Portal for the Italian Strong-Motion Data," *Seismological Research Letters*, **79**(5): 716–722.

Margaris B, Skarlatoudis A, Savvaidis A, Theodulidis N, Kalogeras I and Koutrakis S (2010), "Strong-motion Networks in Greece and Their Efficient Use in the Derivation of Regional Ground Motion Prediction Models," in: S Akkar, P Gülkan, T Van Eck (editors), *Earthquake data in engineering seismology: networks data management and predictive models*, Geotechnical, Geological and Earthquake Engineering Book Series, Chapter 6, Springer, 73–83.

Naeim F (2001), *The Seismic Design Handbook*, Springer, 820.

NERIES Project (2006), "Network of Research Infrastructures for European Seismology," http://www.neries-eu.org/ (Accessed 27 Jan 2010).

Newmark NM and Hall WJ (1982), *Earthquake Spectra and Design, Engineering Monographs on Earthquake Criteria, Structural Design, and Strong Motion Records*, **3**, Earthquake Engineering Research Institute, Oakland, CA.

ORFEUS (2013), "Observatories and Research Facilities for European Seismology," http://www.orfeus-eu.org/ (Accessed in Feb 2013).

Péquegnat C, Guéguen P, Hatzfeld D and Langlais M (2008), "The French Accelerometric Network (RAP) and National Data Center (RAP-NDC)," http://www.rap.obs.ujf-grenoble.fr/ (Accessed 27 Jan 2010).

Péquegnat C, Jacquot R, Gueguen P, Godey S and Frobert L (2011), "Distributed Archive and Single Access System for Accelerometric Event Data: A NERIES Initiative," in: S Akkar, P Gülkan and T Van Eck (editors), *Earthquake Data in Engineering Seismology: Networks Data Management and Predictive Models*, Geotechnical, Geological and Earthquake Engineering Book Series, Chapter 10, Springer, 129–142.

Pitilakis K, Riga E and Anastasiadis A (2012), "Design Spectra and Amplification Factors for Eurocode 8." *Bulletin of Earthquake Engineering*," **10**(5): 1377–1400.

Rey J, Faccioli E and Bommer JJ (2002), "Derivation of Design Soil Coefficients (S) and Response Spectral Shapes for Eurocode 8 using the European Strong-Motion Database," *Journal of Seismology*, **6**: 547–555.

Roca A, Guéguen P, Godey S, Goula X, Susagna T, Péquegnat C, Oliveira CS, Clinton J, Pappaioanou C and Zulfikar C (2011), "The Euro-Mediterranean Distributed Accelerometric Data-Base," in S. Akkar, P. Gulkan and T. Van Eck (editors), *Earthquake Data in Engineering Seismology. Predictive Models, Data Management and Networks*, Geotechnical, Geological and Earthquake Engineering Book Series, Chapter 9, Springer, 115–128.

Rodriguez-Marek A, Bray JD and Abrahamson N (1999), "Task 3: Characterization of site response, General site categories," *Report PEER*, 1999/03.

RRSM (2014), "Rapid Raw Strong Motion system," http://www.orfeus-eu.org/rrsm/information (Accessed in 11 Sept 2014).

Shing TC, Tsai YB, Yeh YT, Lin CC and Wu YM (2003), "Strong Motion Instrumentation Programs in Taiwan," in: Lee W, Kanamori H, Jennings P, Kisslinger C (editors), *International Handbook of Earthquake Engineering Seismology*, Academic Press, International Association of Seismology and Physics of the Earth′s Interior, 1057–1062.

Vilanova SP, Ferreira MA and Oliveira CS (2009), "PAD–1.0 Portuguese Accelerometer Database, CD-rom," *Seismological Research Letters*, **80**(5): 839–844. (in Portuguese)

UBC97 (1997), *Uniform Building Code*, USA.

Wyss A (2004), "Swiss National Strong Motion Network, Strong Motion Bulletin January 2004–December 2004," Available at http://seispc2.ethz.ch/strong_motion/download/Bulletin04.pdf (Accessed 15 Mar 2010).